Tunnelling and Underground Space Technology 82 (2018) 182–190

Contents lists available at ScienceDirect

Tunnelling and Underground Space Technology

journal homepage: www.elsevier.com/locate/tust

Dynamic characteristics research of a ground fissure site at Xi'an, China

Nina Liu[a,b,c,*], Qiangbing Huang[a,b,*], Li Wang[a,b], Wen Fan[a,b], Zikan Jiang[a], Jianbing Peng[a,b]

[a] Key Laboratory of Mine Geological Hazards Mechanism and Control, Chang'an University, Xi'an 710054, China
[b] School of Geological Engineering and Geomatics, Chang'an University, Xi'an 710054, China
[c] Key Laboratory of Western China's Mineral Resource and Geological Engineering, Ministry of Education, Xi'an 710054, China

ARTICLE INFO

Keywords:
Earthquake loading
Ground fissures
Shaking table test
Dynamic response

ABSTRACT

This paper studies the seismic response of an active ground fissure site subjected to earthquake by the shaking table model test. The settlement was induced by the earthquake in the ground fissure site. The settlement increased with the earthquake peak acceleration. The differential settlement has a third-order polynomial relationship with the earthquake intensity. The process of the settlement has three periods, including the rapid deformation stage, the stable deformation stage, and the accelerated development stage. The greatest settlement is in the hanging wall close to the fissure. The secondary fissures and new cracks developed and appeared during the earthquake. The high frequency component of the wave was reduced from the bottom to the top of the site and the low frequency component was amplified. The Fourier amplitude gradual increases correspond to the earthquake acceleration. The results discovery the relationship of subsidence, widen of fissure and the earthquake. It is contribute to the metro design of the fissure area.

1. Introduction

The ground fissure is a kind of geological disaster which is widely spread all over the world. The ground fissures in United States (Holzer, 1984), Mexico (Brunori et al., 2015), Iran (Mohsenin and Hosseinzadeh, 2017), and China (Wang et al., 2016; Peng et al., 2016) have been studied for decades. Most of the ground fissures were discovered by damages they had caused and the former research focused on the original causes for the fissures. The conclusion of the former research is that the main reasons for the fissures both the endogenic and the exogenic causes. The endogenic geological process is the tectonic movement which is caused by the release of energy from the earth's crust. The exogenic process is the physical phenomenon caused by the atmosphere, water, gravity and activity of human beings. Human activity is a partial reason for the development of ground fissures. Human activity changes the earth by various engineering activities, such as the construction of buildings, the withdrawal of groundwater and mining of natural resources.

Historical records indicate that ground fissure have a close relationship with earthquakes. Many historical records show that ground fissures were often only discovered after an earthquake. For example, after the 8.0 Ms earthquake at Huanxian, China in 1556, a lot of ground fissures appeared not only on the surface but the ground also sank 1.0 m below the surface in the Drum-tower district of Weinan city which was in the meizoseismal area. Ground fissures with subsidence were noted again after the 7.5 Ms earthquake in Tongwei, China in 1718 (Zhang et al., 2005). The study of the Haiyuan earthquake (Ms 8.5) which occurred in 1920 also found that loess damage and cracks appearing (Seed, 1968). All of these records show similar characteristics, that is, ground fissures and subsidence appeared together and where more ground fissures were observed, more subsidence was also observed.

In order to get the relationship between earthquake and ground fissures, lots of research has been done through field surveys, model tests and so on. Wang studied dynamic characteristics of the loess plateau by the shaking table test and the numerical analysis. Lots of cracks appeared on the surface of the model site and the amplification effect was observed during the earthquake process. With the increase of loess plateau height, acceleration, velocity, and the displacement were amplified. With the propagation of the earthquake wave, the low-frequency component increased and was the predominant frequency, while the high-frequency component was absorbed and decreased (Wu et al., 2013; Wang and Wu, 2017).

The relationship between earthquakes and ground fissures has been studied not only in China but in other countries of the world. Dobrev and Kost'ak found that during earthquakes, the monitoring point located in a fissure of the Struma fault zone became increasingly active (Dobrev, 2000). The research field was located in southwest Bulgaria within the epicentral zone which was one of the strongest earthquakes

* Corresponding authors at: School of Geological Engineering and Geomatics, Chang'an University, Xi'an 710054, China.
E-mail addresses: dcdgx16@chd.edu.cn (N. Liu), dcdgx24@chd.edu.cn (Q. Huang).

https://doi.org/10.1016/j.tust.2018.08.044
Received 4 October 2017; Received in revised form 6 May 2018; Accepted 17 August 2018
0886-7798/ © 2018 Elsevier Ltd. All rights reserved.

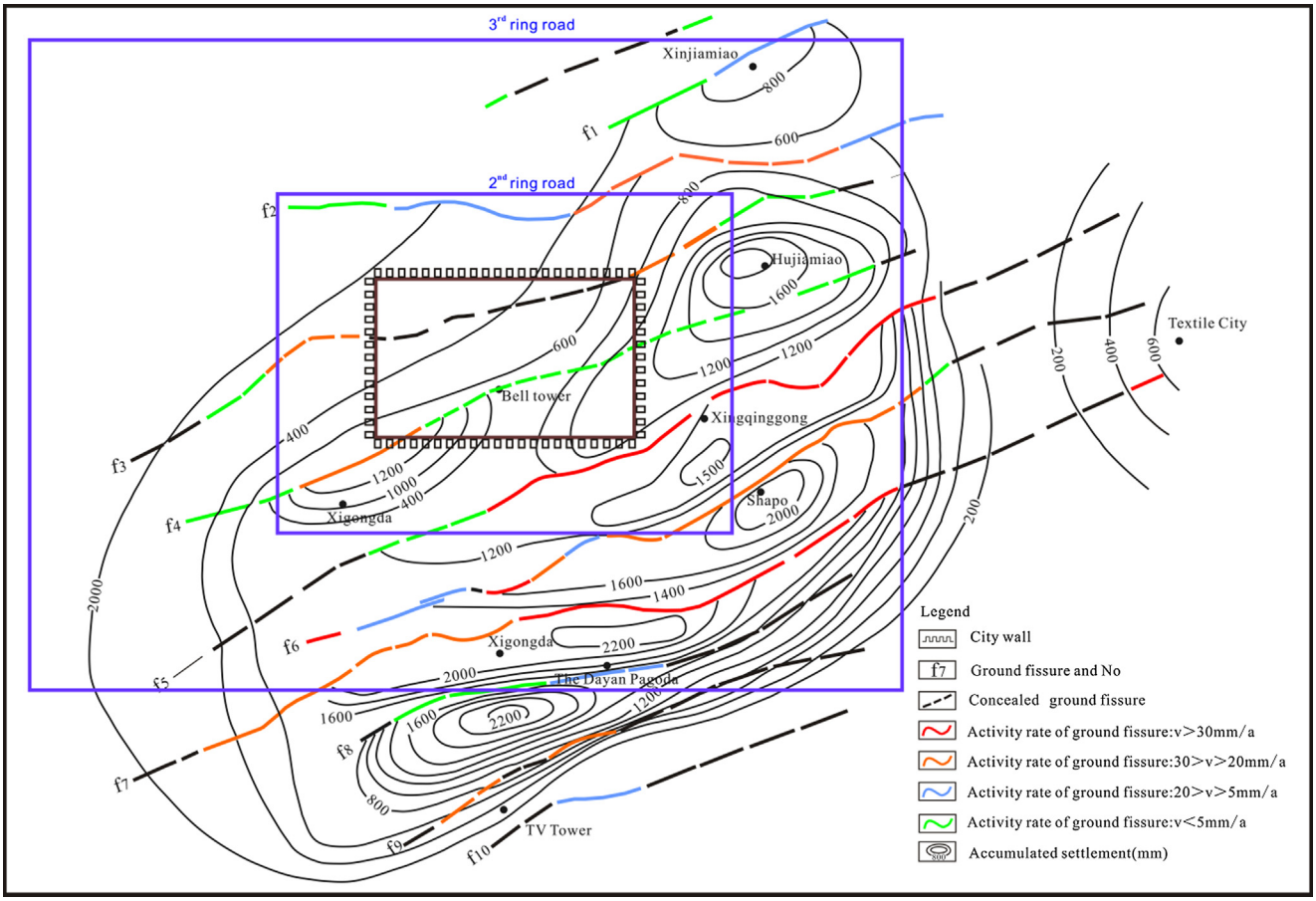

Fig. 1. Layout of ground fissures and subsidence in Xi'an.

in Europe. Researchers also found that the earthquake is a partial reason for ground fissure formation (Alessandro, 1999). Irene studied the formation of ground cracks in the earthquake in India. Cracks were formed in the dynamic process of the Chamoli earthquake. Just prior to the earthquake, under the influence of the local ambient stress field, the ground at these sites was already close to tension failure. When an earthquake wave was passing through the geographic region, the stress perturbations across the planes of the cracks were induced. The Chamoli earthquake led to the formation of tensile cracks (Sarkar, 2004). Muneo and Navaratham studied the propagation of smoothly growing cracks caused by the large deformation of earthquake faults in Japan. They observed that the cracks originated from and were propagated by earthquakes (Hori and Vaikunthan, 1998). From the field survey, the conclusion can be made that ground fissures have a close relationship with earthquakes.

Based on the field survey, prototype models were set and equipment was used to study the dynamic characteristics of ground fissures (Liu et al., 2017; Kang et al., 2016; Kang and Kang, 2015; Wang et al., 2015). The shaking table is a useful seismic simulation system for providing subtlety of loading, easy control and successful data recording (Pitilakis et al., 2008; Chen and Shen, 2014). It has been used to conduct the dynamic response and failure mechanisms of soil and structure interaction in various seismic activities (Chen et al., 2016; Sun et al., 2011).

Xi'an is the capital city of Shaanxi Province and the economic center of northern China. The economic and politics important development require the safety and the stability of the city. Recently the city developed quickly with many underground structures particularly the metro. However 14 ground fissures spread all over the city have been surveyed in the past 20 years, Xi'an city has records of strong earthquakes in its history. It is located within the strongest earthquake area of China. The metro tunnels however intersect with many ground fissures. It is essential to understand the relationship between earthquakes, subsidence and ground fissure activities to make sure the metro is safe in the 100 years. This research is focused on the dynamic characteristics of the ground fissure site when it is subjected to the load of an earthquake. The shaking table test was conducted based on the field survey. The subsidence process, the fissure propagation, and the earthquake wave characteristics were observed, compared and analyzed. The results will help with the city planning not only in Xi'an City but also cities such as Beijing and Wuxi, where fissures appear.

2. Subsidence and damage caused by ground fissures

2.1. Ground fissures in China

The ground fissures are distributed in more than 16 provinces of China. The most serious areas influenced by the ground fissure are northern China and the Yangtze Delta. According to a 2012 report, the economic loss caused by fissures has already exceeded 10 billion RMB Yuan in China. Numerous ground fissures have been found in field surveys. For example, the number of ground fissures is up to 103 in Taiyuan Basin, 86 in Fenwei basin, 106 in Yuncheng Basin, 212 in Weihe basin. The total number discovered is above 500, but this accounts for only a small percent of China'a total fissures.

These fissures not only influence the safety of existing buildings but also limit urban planning. The cities most influenced by fissures are Beijing, Xi'an, Suzhou, Wuxi and Changzhou. In Beijing, the ground fissures occur in Changping district, Shungyi district and Haidian district. The high-speed railways, the natural gas pipelines and houses are seriously threatened by the ground fissures in these three districts. Xi'an city is seriously influenced by fissures too. The total number is 14

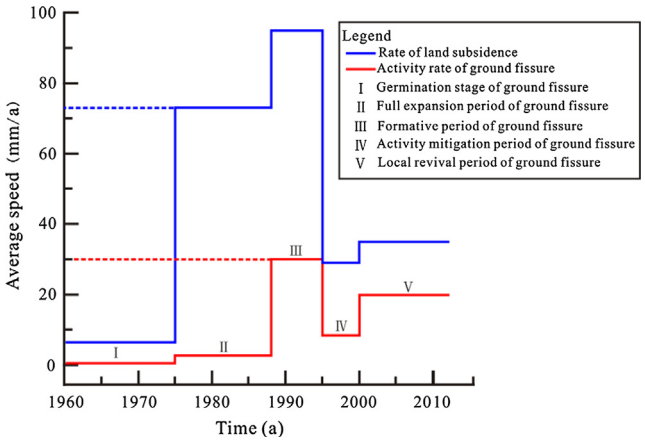

Fig. 2. Mean velocity of ground fissures and subsidence in Xi'an.

Fig. 3. Settlement of highway ramp in a ground fissure site.

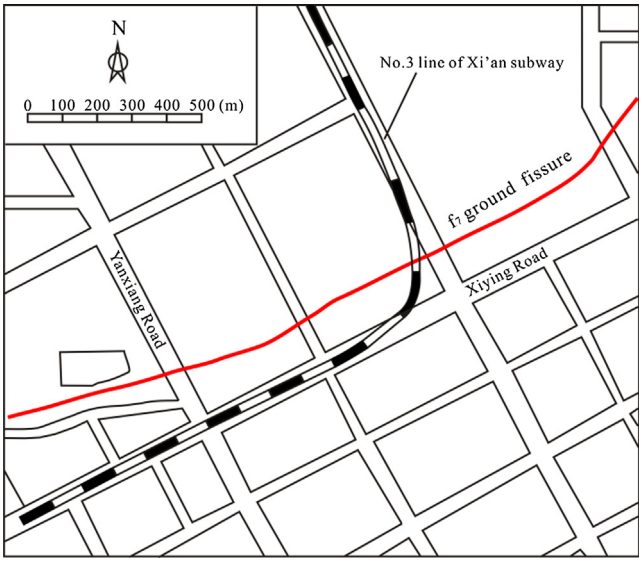

Fig. 4. Plane distribution of ground fissures f_7 near the metro line YK26 + 850.

covering an area of 150 km^2 almost the whole city. The subsidence caused by fissures led to the leaning of buildings, the uneven settling of intersections and the breakage of water supply systems in the Xi'an city. Suzhou, Wuxi and Changzhou are all threaten by the subsidence and ground fissures. The total subsidence of the three cities is more than 1200 mm, and the stretch of the fissures in this area was 8.8 mm/a in 2012 (Lu et al., 2014; Zhu et al., 2007).

Table 1
Main performance parameters of shaking table.

Performance index	Parameter		Performance index	Parameter	
Platform size	4 m × 4 m		Maximum overturning moment	80 t·m	
Test frequency	0.1–50HZ		Maximum eccentric moment	30 t·m	
Maximum load	30 t		Shaking direction	X, Y, Z	
Maximum acceleration	X direction	± 1.5 g	Maximum displacement	X direction	± 15 cm
	Y direction	± 1.0 g		Y direction	± 25 cm
	Z direction	± 1.0 g		Z direction	± 10 cm

Fig. 5. Shaking table control system.

2.2. Relationship of subsidence and ground fissures

From the historic record and field survey, it was found that the velocity of subsidence is often associated with the velocity of ground fissures, and the subsidence is the most obvious disaster caused by ground fissures. Fig. 1 shows the layout of subsidence and ground fissures within Xi'an city. The severe subsidence areas correspond with the fields where severe ground fissure activity occurs. For example, the accumulated subsidence in the south part of the city is as high as 2200 mm. This area is really close to fissures f_7, f_8 and f_9. The mean velocity of these three fissure activities is about 20–30 mm per year in this area. The activities of subsidence and fissures both are greater than those of other parts in Xi'an.

Fig. 2 shows the velocity of the subsidence and that of the ground fissures in the past 50 years of Xi'an city. According to the activities of fissures, the time is divided into five periods: germination stage (I), full expansion period (II), formative (III), activity mitigation (IV) and revival period (V). The rate of land subsidence corresponds closely with the fissures activities. There were four periods where ground fissures had serious activity as 1975–1988 (II), 1988–1995 (III), 1995–2000 (IV), 2000-now (V). In the first period (I), the year before 1975, few ground fissures appeared and their activities were usually overlooked. From 1975 to 1988 (II), the subsidence velocity was 72 mm per year. It increased about 64 mm from the first period (I). The main reason for the fast increase was the withdrawal of ground water which began in 1975. From 1988 to 1995 (III), the subsidence and fissures activities peaked. The speed of subsidence was almost 98 mm each year. And in this period, the ground fissure activity increased from 2 mm to 30 mm each year. Realizing the serious threat from the subsidence, a couple of policies were implemented forbidding the withdrawal of ground water. As a result of the policies the speed of subsidence and ground fissure activity both began to decrease after 1995. In the year 2000, the subsidence and ground fissure activity both increased slightly. Since that time their velocities have remained the same for about 17 years. Thus

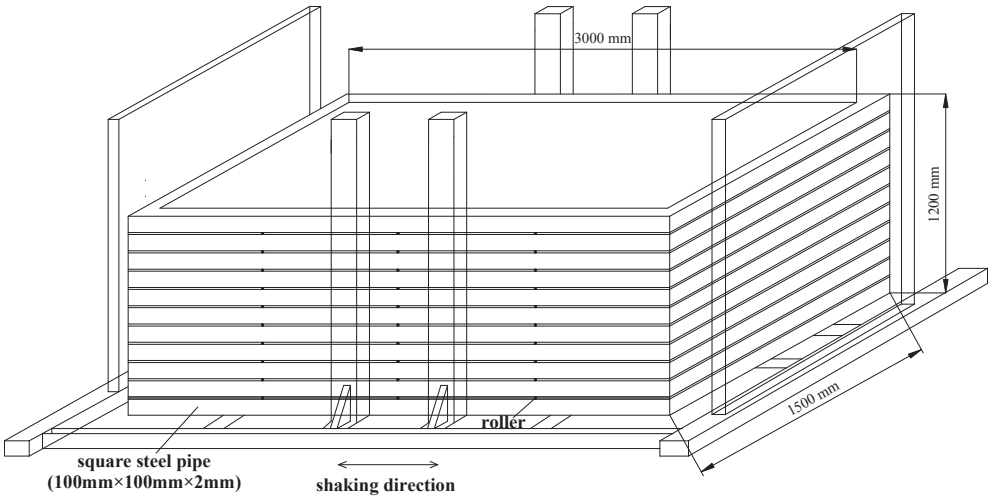

(a) Design of model box

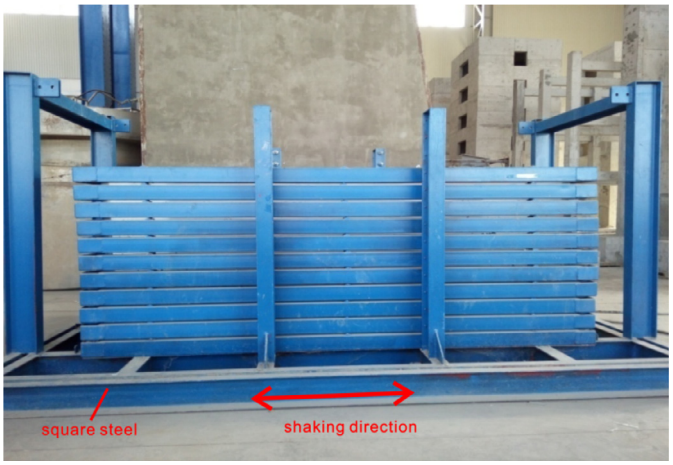

(b) Model box

Fig. 6. Diagram of model box.

Fig. 7. Treatment of friction at the box bottom.

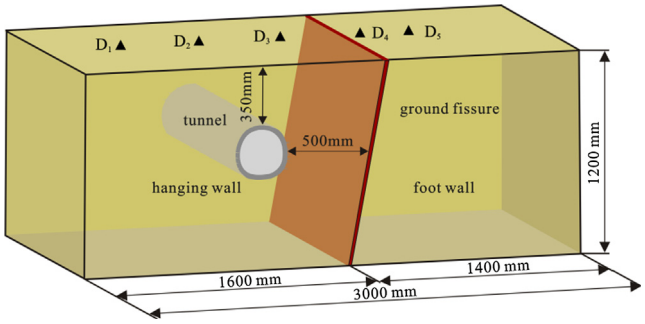

Fig. 8. Rendering of the model.

Fig. 2 shows a clear correspondence between the subsidence and the ground fissure activity of with Xi'an city.

2.3. Damage caused by ground fissures

Since 1975, damages to buildings, roads and overpass, as well as other structures have occurred. Fig. 3 shows a ramp breakage on Xi'an Ring Road III where the road intersects with ground fissure f_{10}. The vertical displacement between the hanging wall and foot wall of the fissure on the road surface is up to 60 mm. The uneven settlement of the road is a serious threat to road safety.

To ensure safety, city code of forbids building on an area where ground fissures activity occurs. But linear engineering such as highways or subways, it is difficult to avoid all 14 ground fissures in the city. Most of the roads and subways intersect with the ground fissures activity or run closely parallel to the fissures. For example, the Metro Tunnel I cross 5 ground fissures in 8 sites, the Ring Road II crosses ground fissure f_6 in the Chang'an Intersection, the Metro Tunnel III closely parallels to several ground fissures at its west and east ends.

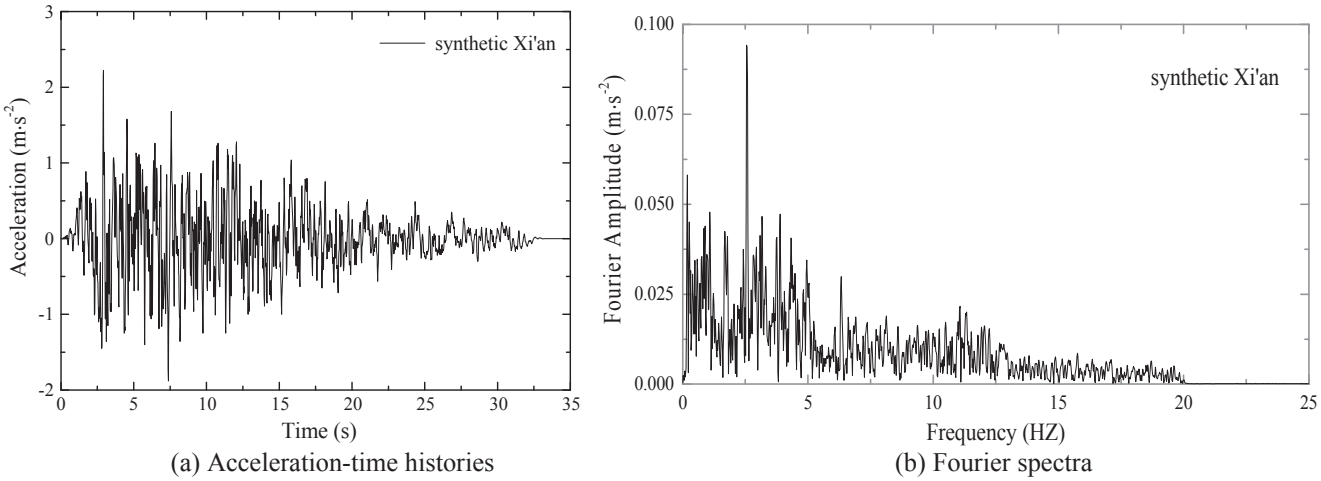

(a) Acceleration-time histories (b) Fourier spectra

Fig. 9. Synthetic Xi'an earthquake wave.

(a) Acceleration transducer (b) Mini earth pressure sensor (c) strain gauge

Fig. 10. Test instrumentations.

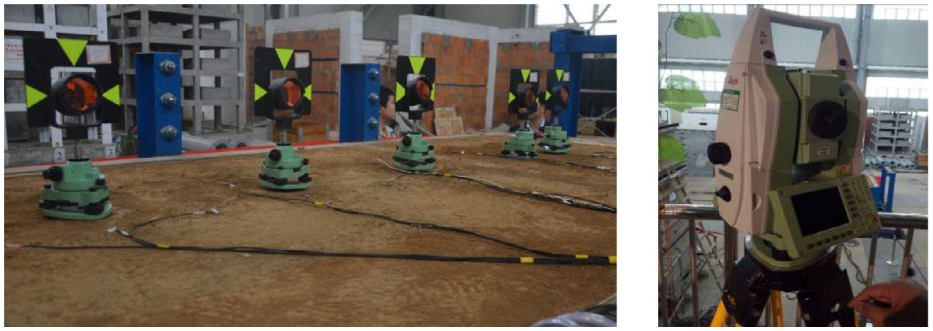

(a) The distribution of circular prism (b) Leica TS30 measuring robot

Fig. 11. Surface subsidence displacement monitoring.

2.4. Relationship of earthquake and ground fissure

Based on the research in the past 20 years, we know the reasons for the ground fissures in Xi'an. The original reason is complex. The geological structure is the controlling reason which leads to the origin and development of ground fissures. The geological stress determines the direction of the ground fissures. The withdrawal of groundwater triggers the fissure and the sinking water level expands the fissure. The earthquake usually leads to the sharp stress change in a short time. The stress caused by earthquakes influences not only ground fissures but the subsidence in the fissure area.

3. Model design

3.1. Prototype

Xi'an subway III runs closely parallel to the ground fissure f_7 at the site of YK26 + 850 Fig. 4). The landscape of this area is flat, where the ground elevation is 409.46–441.43 m. The geomorphic unit is loess ridge and depression. The subway tunnel in the area is of 10–15 m below surface. The stratum has 4 layers from the surface to the bottom of the subway tunnel. The 4 layers of the stratum are the postglacial epoch artificial earth fill (Q_4^{ml}), upper pleistocene aeolian loess (Q_3^{eol}), residual palaeosolic (Q_3^{el}), and middle pleistocene alluvial silty clay (Q_2^{al}) from top to bottom.

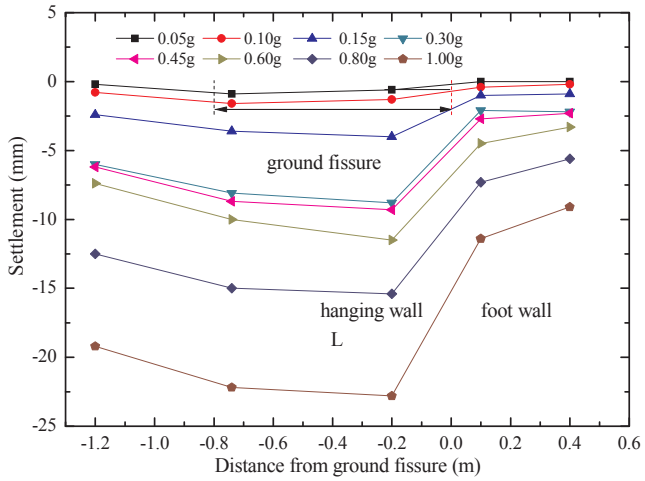

Fig. 12. Subsidence curve of ground fissure site.

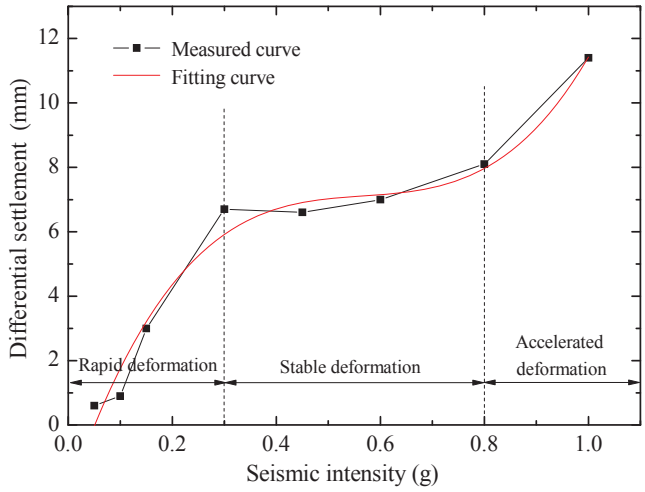

Fig. 13. Subsidence curves in seismic intensity near ground fissures.

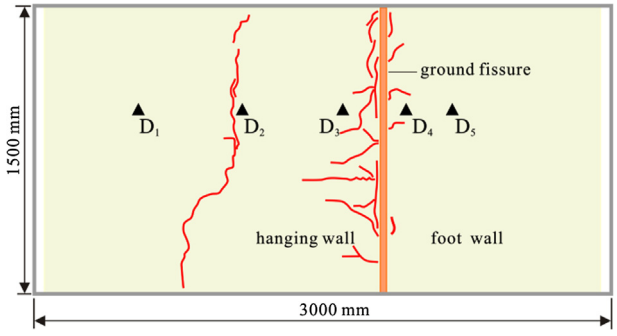

Fig. 14. Sketch of cracks on the site surface.

3.2. The shaking table and model box

The shaking table is a common testing method for studying seismic performance of various site and underground structures (Chen and Shen, 2014; Chen et al., 2016; Sun et al., 2011; Lu et al., 2014). In the shaking table tests, the flexible, shear stack or rigid containers have often been utilized for simulating different boundary conditions (Zhu et al., 2007). The model box is fixed on the table and loads the seismic activities by the controlling system. Table 1 shows the parameters of the system in detail. Fig. 5 shows the controlling system of the shaking table.

The model test uses a laminar shear model box for its high ability to of minimize boundary effects. The size of the model box is 3.0 m (length) × 1.5 m (width) × 1.2 m (height). The laminar shear model box has steel plates connected to the outside of the box to prevent the laminar structures from creeping down during the seismic duration. The laminar box has a total of 11 layers, with each layer 12 mm apart. The laminar structure is made of hollow square steel pipe. The size of the steel pipe is 100 mm (length) × 100 mm (width) × 2 mm (height). Three grooves are in each side of the steel pipe. Steel balls with lubricating oil are in the grooves. The balls can help the free sliding of each layer. Fig. 6(a) is the structure design of the model box and Fig. 6(b) is the picture of the model box prepared in detail for the experiment.

The model box design considers 3 boundary effects. They are the sliding boundary which is parallel to the shaking direction, the flexible boundary which is perpendicular to the shaking direction and the friction boundary at the bottom of the model box. The sliding boundary is made of rubber film and is 0.8 in. thick. The lubricating oil is inside of the rubber film. It is designed to make sure the sliding boundary can decrease the friction between the model box and soil. The rubber film is essential for preventing soil and water leaking away. The flexible boundary's polystyrene foam board, which is 50 mm thick, is to absorb the wave reflection. The friction boundary prevents slippage between the box bottom and the soil is against the relative slip. To make the bottom coarse wood treads were embedded in order to create enough friction to hold the soil. Each tread has 300 mm distance from each others. The total number of the wood treads is 9. Fig. 7 shows the wood treads at the bottom of box.

3.3. Simulation of the ground fissure and the site

In the dynamic experiment, it is hard to simulate all characteristics of the soil. Usually main characteristics and similarity rules are considered in the shaking table test. The soil of the test is taken from the subway construction site located in the ground fissure site. After the impurity of the soil is removed, the soil is sifted by a 10 mm screen mesh, and then compacted in the model box, layer by layer. Each layer surface of the soil is roughened by a steel brush to keep all layers connected together. In compacting the soil, the water constant and the density of the soil are controlled to replicate the construction site. The fissure is filled with fine sand similar to sand found in the construction site. Its 80^0 trend is the same as found in the metro tunnel construction site. Fig. 8 shows the model of the ground fissure site.

3.4. Data acquisition system

In the shaking table test, the earthquake simulation is important to ensure accuracy and applicability. The synthetic Xi'an earthquake follows the geological characteristics of the region. Fig. 9(a) shows the acceleration and time history while Fig. 9(b) shows Fourier spectra and frequency of the synthetic Xi'an earthquake wave.

The monitoring equipments of the shaking table test are essential. The model test has a various kinds of equipment for the process of earthquake loading. The YD-31D acceleration transducer records accelerations, strains and soil pressures, with the help of ZFCY380 which is a piezoelectric type mini soil pressure sensor and BX120-5AA (50 mm × 3 mm) which is a strain gauge (Fig. 10). The subsidence of the model surface is monitored by the Leica TS30 robot measuring system, with the Leica round prisms buried in the site (Fig. 11). The total number of Leica round prisms is 5. There are 3 prisms buried in the hanging wall marked as D1–D3, and 2 prisms buried in the foot wall marked as D4 and D5 Fig. 8.

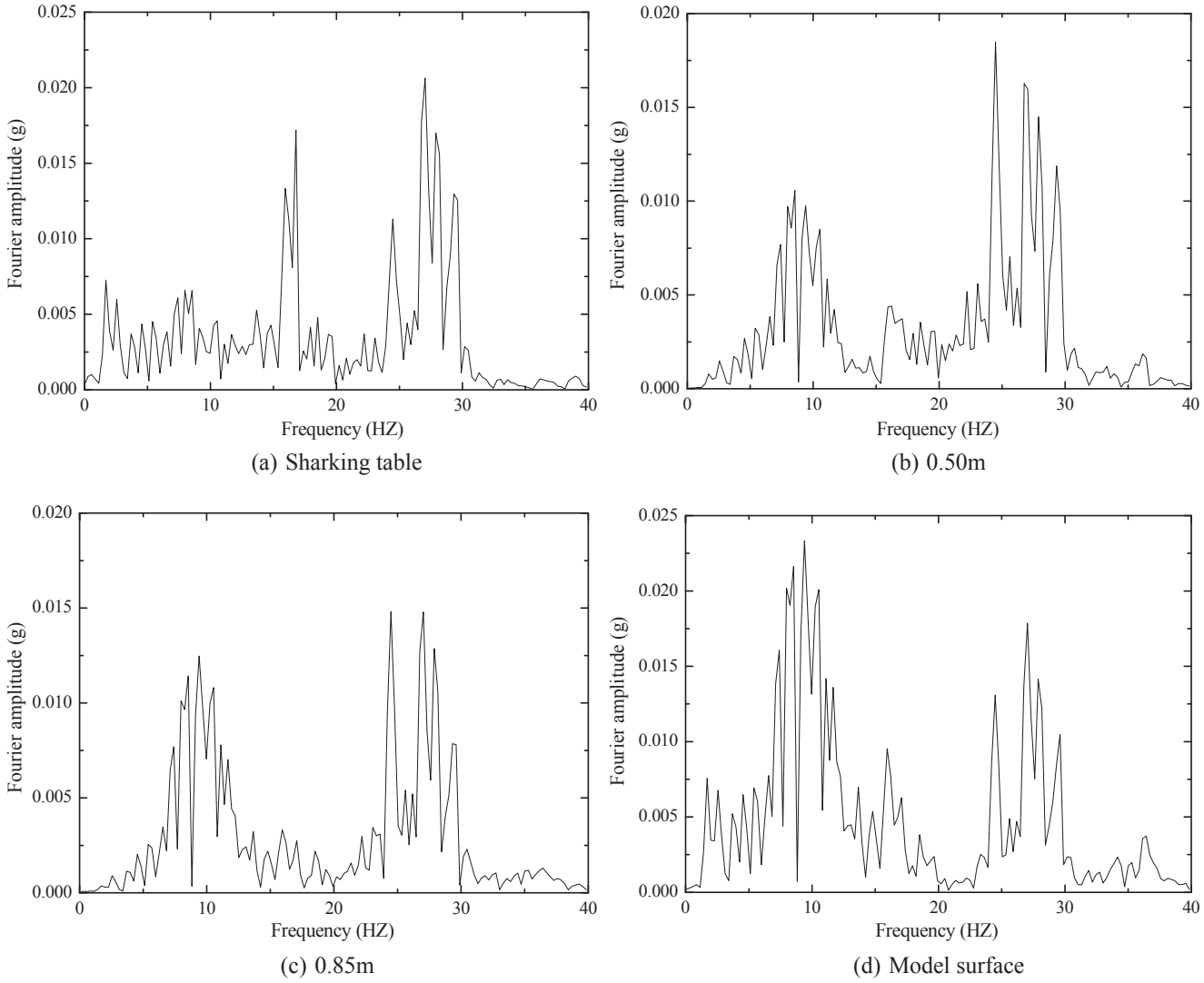

Fig. 15. Fourier spectrum of partial measuring points of ground fissure's hanging wall (0.15 g).

4. Result and analysis

4.1. Subsidence of the site

Fig. 12 shows the subsidence curves of the model surface when the synthesis Xi'an earthquake waves were applied through the shaking table with peak acceleration from 0.05 g to 1.00 g. The curves indicate that the earthquake leads to the subsidence of the ground fissure site. The setting in hanging wall and the foot wall were different. The hanging wall had more subsidence than that of the foot wall. The pattern observed both on the hanging wall and the foot wall was that subsidence occurred at a greater rate the closer it was to the fissure. The higher the peak acceleration of the earthquake wave, the more subsidence occurred on the site surface. The greatest settlement was on the hanging wall close to the fissure, where the subsidence was up to 22.8 mm at the peak acceleration (1.00 g).

The typical traction deflection character is clear between the hanging wall and the foot wall. The traction deflection is caused by the differential settlement on both sides of the fissure. In the hanging wall, a distance of 0.8 m from the fissure shows the greatest subsidence. This distance is the major deformation zone. Outside this range, the settlement is less.

Fig. 13 shows the differential settlement between the hanging wall and the foot wall on both side of the fissure according with the seismic intensity. The measured curve indicates a strong correlation between seismic intensity and differential settlement. The differential settlement is increases with seismic intensity. The fitting curve shows the relationship between the differential settlement and earthquake intensity as:

$$\Delta H = mA^3 + nA^2 + pA + q$$

ΔH stands for the differential settlement between the hanging wall and the foot wall;
A stands the seismic intensity;
M, n, p and q are parameters of the settlement curve, and all of them are constants.

The mean square deviation of the formula is 0.96 which shows the fitting is highly accurate. The formula indicates that the differential settlement (ΔH) has a three polynomial equation relationship with the seismic intensity (A).

The observation record, measured curves and the fitting curve indicate that the settlement process has three periods. In the rapid deformation stage, the earthquake intensity is less ($A \leq 0.3$ g), the differential settlement between the hanging wall and the foot wall increases quickly, and the fissure appears on the surface of the site. In the stable deformation stage, the curve of the differential settlement is flattened ($0.3\text{ g} < A \leqslant 0.8\text{ g}$) indicating the subsidence rate of the fissure

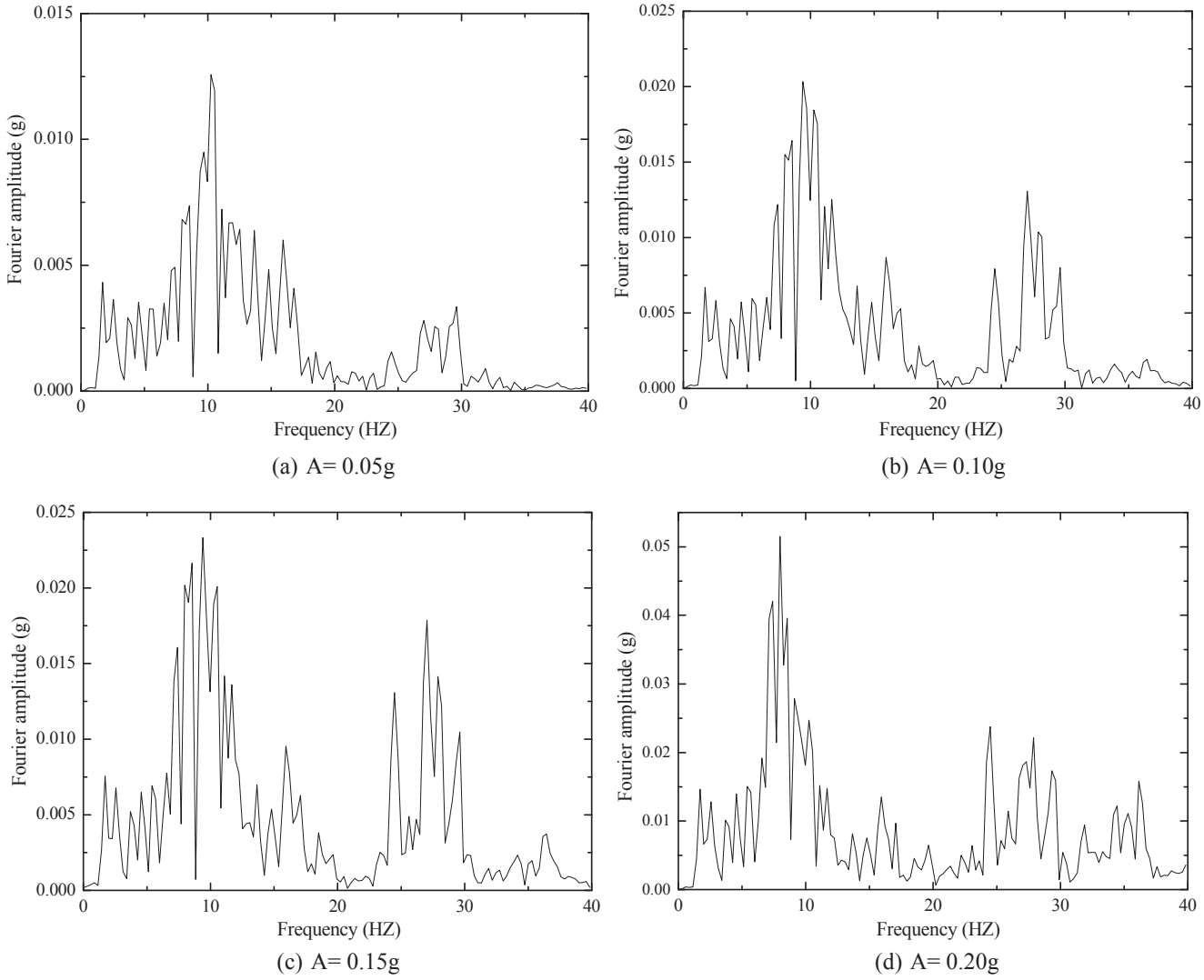

Fig. 16. Fourier spectrum of surface test point in synthesis Xi'an wave.

site is low. In the accelerated development stage, the differential settlement (A>0.8 g) between the hanging wall and the foot wall increases rapidly and the cracks in the fissure widen. The three stages indicate the relationship between the seismic intensity and the differential settlement.

4.2. Ground cracks and failure

During the seismic activity process of the test, the tension cracks appeared on the surface of the model site. The differential settlement between the hanging wall and the foot wall increased Fig. 14). The width of the main fissure increased. The secondary fissure appeared closely parallel to the main fissure on the surface of the hanging wall. The width of the secondary fissure was 4–8 mm. Many small cracks appeared in the hanging wall intersecting the main fissure at right angles. The width of these cracks were 1–3 mm. The widening of the new cracks, the main fissure and the secondary fissure as well as the steep displacement between the hanging wall and the foot wall could potentially lead to the damage of the ground fissure site.

4.3. Frequency domain characteristic

The Fourier spectrum characteristic of the earthquake wave changed a lot when it was spread in the soil. From the data recorded during the loading of the seismic activity, the Fourier spectrum of accelerations was analyzed. Fig. 15 shows the Fourier spectrum of accelerations recorded in each of the four points of the model box when the shaking table loaded the synthesis Xi'an wave with acceleration of 0.15 g. Fig. 15(a) is the shaking table surface, Fig. 15(b) is 0.50 m above the surface, Fig. 15(c) is 0.85 m above the surface, and Fig. 15(d) is the top of the model site. Fig. 15 shows that the predominant frequency of the earthquake waves was concentrated in ranges as 15–17 Hz and 24–30 Hz on the surface of the shaking table. The predominant frequency was concentrated in 7–12 Hz and 24–30 Hz at a height of 0.50 m, 0.85 m and the surface of the site.

The spectrum characteristic changed from the bottom to the surface in the model site. Comparing the Figures (b), (c) and (d), one can see that with the increase of the height, the Fourier amplitude frequency concentrated in 7–12 Hz increased from 0.01 g to 0.023 g, while the Fourier amplitude frequency concentrated in 24–30 Hz decreased a little from 0.19 g to 0.16 g. The result indicates that when the earthquake wave spread in the ground fissure site from bottom to top, the high frequency component of the wave was reduced, and the low frequency component was amplified.

Fig. 16 shows the Fourier spectrum on the surface of the hanging wall when loading synthesis Xi'an wave in the earthquake acceleration as 0.05 g, 0.10 g, 0.15 g and 0.20 g. With the increase of the earthquake acceleration from 0.05 g to 0.20 g, the amplify effect is increasing.

Fig. 16 indicates a gradual increase of the Fourier spectrum as show below: 0.0125 g (Fig. 16(a)), 0.020 g (Fig. 16(b)), 0.023 g (Fig. 16(c)), and 0.05 g (Fig. 16(d)). The Fourier amplitude increasing ratio corresponds to the earthquake acceleration. As the acceleration increases, the earthquake intensity increases as well. The nonlinear residual deformation of the soil increases and the rigidity of the soil decreases. These factors lead to the predominant frequency decreasing and the Fourier spectrum increasing.

5. Conclusion and discussion

(1) The settlement was induced by the earthquake in the ground fissure site. The settlement increased with the earthquake peak acceleration. The differential settlement has a third-order polynomial relationship with the earthquake intensity. The process of the settlement has three periods, including the rapid deformation stage, the stable deformation stage, and the accelerated development stage. The greatest settlement is in the hanging wall close to the fissure. Settlement decreases with distance away from the fissure both in the hanging wall and the foot wall.
(2) The secondary fissures and new cracks developed and appeared during the earthquake. The secondary fissure was exposed in the hanging wall and it was parallel to the main fissure. Some new cracks appeared on the surface of the hanging wall and intersected the main fissure at right angles. The width of the main fissure was the greatest (about 10 mm), the width of the secondary fissure was less (5–8 mm), while the width of the cracks was 1–3 mm.
(3) The high frequency component of the wave was reduced from the bottom to the top of the site and the low frequency component was amplified. The Fourier amplitude gradual increases correspond to the earthquake acceleration.

From the shaking table test the dynamic characteristics of ground fissure site have been studied. The results carry forward the former research and conclude a relationship between the differential settlement and earthquake intensity. These results are useful in metro design protection of safety. More research is still needed on the dynamic characteristic of the tunnel located in the fissure area, as well as the stress and strain of the tunnel where different subsidence within the hanging wall and the foot wall of the ground fissure occurs. Based on the results from the research, further work will be applied.

Acknowledgements:

This research was supported by the National Natural Science Foundation of China (41502277, 41772274, 41630634), the Fund of Key Laboratory of Mine Geological Hazards Mechanism and Control (2017KF06), the Special Fund for Basic Scientific Research of Central Colleges, Chang'an University (300102268502) and the National Basic Research Program of China (973 Program: 2014CB744700). All supports are gratefully acknowledged.

References

Holzer, T.L., 1984. Ground failure induced by ground-water withdrawal from unconsolidated sediment. Geol. Soc. Am. Rev. Eng. Geol. 6, 67–102.
Brunori, C., Bignamic, C., Albano, M., et al., 2015. Land subsidence, Ground Fissures and Buried Faults: InSAR Monitoring of Ciudad Guzmán (Jalisco, Mexico). Remote Sensing 7 (7), 8610–8630. https://doi.org/10.3390/rs70708610.
Mohsenin, S.A., Hosseinzadeh, S.R., et al., 2017. Variations in spatial patterns of soil–vegetation properties over subsidence-related ground fissures at an arid ecotone in northeastern Iran. Environ. Earth Sci. 76 (6), 234. https://doi.org/10.1007/s12665-017-6559-z.
Wang, G.Y., You, G., Zhu, J.Q., et al., 2016. Earth Fissures in Su–Xi–Chang Region, Jiangsu, China. Surv. Geophys. 1–22. https://doi.org/10.1007/s10712-016-9388-9.
Peng, J.B., Qiao, J.W., Leng, Y.Q., et al., 2016. Distribution and mechanism of the ground fissures in Wei River Basin, the origin of the Silk Road. Environ. Earth Sci. 75 (8), 1–12. https://doi.org/10.1007/s12665-016-5527-3.
Zhang, Z.Z., Zhang, D.L., Liu, H.M., 2005. Comprehensive study on seismic subsidence of loess under earthquake. Northwest Seismol. J. 27 (1), 36–41.
Seed, H.B., 1968. Landslide during earthquake due to soil liquefaction. J. Soil Mech. Found. Div., ASCE 94 (5), 1055–1122.
Wu, Z.J., Wang, L.M., Wang, P., et al., 2013. Influence of site conditions on ground motion at far field loess sites during strong earthquake. J. Central South Univ. 20 (8), 2333–2341. https://doi.org/10.1007/s11771-013-1741-2.
Wang, L.M., Wu, Z.J., 2017. Effects of site conditions on earthquake ground motion and their applications in seismic design in loess region. J. Mountain Sci. 14 (6), 1185–1193. https://doi.org/10.1007/s11629-016-3921-7.
Dobrev, N.D., Kost'ak, B., 2000. Monitoring tectonic movements in the Simitli Graben, SW Bulgaria. Eng. Geol. 57, 179–192.
Alessandro, B., 1999. The March 1981 Mount Etna eruption inferred through ground deformation modelling. Phys. Earth Planet. Inter. 112, 125–136. https://doi.org/10.1016/S0031-9201(99)00003-5.
Sarkar, I., 2004. The role of the 1999 Chamoli earthquake in the formation of ground cracks. J. Asian Earth Sci. 22, 529–538.
Hori, M., Vaikunthan, N., 1998. Analysis of smooth crack growth in brittle materials. Mech. Mater. 28, 33–52. https://doi.org/10.1016/S0167-6636(97)00053-7.
Liu, N., Huang, Q.B., Ma, Y.J., et al., 2017. Experimental study of a segmented metro tunnel in a ground fissure area. Soil Dyn. Earthq. Eng. 100, 410–416. https://doi.org/10.1016/j.soildyn.2017.06.018.
Kang, X., Ge, L., Chang, K.T., et al., 2016. Strain-controlled cyclic simple shear tests on sand with radial strain measurements. J. Mater. Civ. Eng. 28 (4), 04015169. https://doi.org/10.1061/(ASCE)MT.1943-5533.0001458.
Kang, X., Kang, G.C., 2015. Modified monotonic simple shear tests on silica sand. Mar. Georesour. Geotechnol. 33 (2), 122–126. https://doi.org/10.1080/1064119X.2013.805289.
Wang, Z.Z., Jiang, Y.J., Zhu, C.A., 2015. Shaking table tests of tunnel linings in progressive states of damage. Tunn. Undergr. Space Technol. 50, 109–117. https://doi.org/10.1016/j.tust.2015.07.004.
Pitilakis, D., Dietz, M., Wood, D.M., 2008. Numerical simulation of dynamic soil-structure interaction in shaking table testing. Soil Dyn. Earthq. Eng. 28 (6), 453–467. https://doi.org/10.1016/j.soildyn.2007.07.011.
Chen, Z.Y., Shen, H., 2014. Dynamic centrifuge tests on isolation mechanism of tunnels subjected to seismic shaking. Tunn. Undergr. Space Technol. 42, 67–77. https://doi.org/10.1016/j.tust.2014.02.005.
Chen, Z., Chen, W., Li, Y., 2016. Shaking table test of a multi-story subway station under pulse-like ground motions. Soil Dyn. Earthq. Eng. 82, 111–122. https://doi.org/10.1016/j.soildyn.2015.12.002.
Sun, T., Yue, Z., Gao, B., Li, Q., 2011. Model test study on the dynamic response of the portal section of two parallel tunnels in a seismically active area. Tunn. Undergr. Space Technol. 26, 391–397. https://doi.org/10.1016/j.tust.2010.11.010.
Lu, Y., Shi, B., Xi, J., et al., 2014. Field study of Botdr-based distributed monitoring technology for ground fissures. J. Eng. Geol. 22 (1), 8–13. https://doi.org/10.13544/j.cnki.jeg.2014.01.001. (in Chinese).
Zhu, L., Su, X.S., Duan, F.Z., et al., 2007. Virtual simulation of ground subsidence in Suzhou-Wuxi-Changzhou region. J. Nat. Disasters 6 (1), 136–140 (in Chinese).